J|A|C|S COMMUNICATIONS

Published on Web 07/12/2010

Carrier-Tunable Magnetic Ordering in Vanadium−Naphthalene Sandwich Nanowires

Zhuhua Zhang,[†,‡] Xiaojun Wu,[‡,§] Wanlin Guo,*[,†] and Xiao Cheng Zeng*[,‡]

Institute of Nano Science, Nanjing University of Aeronautics and Astronautics, Nanjing 210016, China, Department of Chemistry, University of Nebraska−Lincoln, Lincoln, Nebraska 68588, and Department of Materials of Science and Engineering, University of Science and Technology of China, Hefei 230026, China

Received April 6, 2010; E-mail: wlguo@nuaa.edu.cn; xczeng@phase2.unl.edu

Abstract: We report results of first-principles calculation of novel $NpTM_2$ (Np = naphthalene; TM = V, Mn, Ti, Nb) sandwich nanowires. Most importantly, we find that the magnetic ordering in the NpV_2 nanowire can be adjusted by changing its charge state. Its intrinsic antiferromagnetic ordering can be switched to ferromagnetic ordering by injecting electrons, whereas injecting holes to the nanowire can further stabilize the antiferromagnetic state. This carrier-tunable magnetic ordering appears to be unique to the NpV_2 nanowire. Moreover, we find that the bonding between the two nearest-neighbor metal atoms plays a key role in controlling the magnetic coupling of charge-neutral $NpTM_2$ nanowires. We predict that the $NpMn_2$ nanowire is ferromagnetic while the $NpTi_2$ and $NpNb_2$ nanowires are antiferromagnetic.

Organometallic sandwich nanowires (SWNs) have recently undergone a flurry of research interest due to their intriguing nanostructures and promising potential for future spintronic applications.[1−15] A key property of magnetic SWNs lies in the strong coupling of local magnetic moments in the nanowire direction. In magnetic SWNs, the magnetic coupling between axially adjacent metal atoms can be ferromagnetic (FM), paramagnetic (PM), or antiferromagnetic (AFM), depending on the electron configuration of the metal elements as well as the properties of the ligand molecules.[1,16] For practical applications, it would be desirable to synthesize SWNs with tunable magnetic coupling, as they can afford greater flexibility in design and optimization of nanodevices. However, how to regulate the magnetic coupling of magnetic SWNs to achieve such tunability is still little explored.

A naphthalene ($Np = C_{10}H_8$) molecule can be viewed as two fused benzene (Bz) rings. Previous experimental and theoretical studies have demonstrated that two parallel Np molecules can encompass metal atoms, such as V and Ti, to form stable sandwich configurations.[17−20] A series of Np_nV_m clusters with presumed multiple-decker structures, such as Np_3V_4 and Np_4V_6, have been synthesized.[21] Hence, it is conceivable that the $NpTM_2$ SWNs, with each unit cell consisting of one Np molecule and two metal atoms, can be synthesized in the laboratory. In this Communication, we show evidence from first-principles calculation that an NpV_2 SWN not only is highly stable but also entails carrier-tunable magnetic ordering. We find that injecting electrons into the nanowire can switch its intrinsic AFM ordering to FM ordering, whereas injecting holes can substantially stabilize the AFM phase. This unique switching mechanism arises from carrier-mediated exchange coupling between the V 3d orbitals. In addition, a hole-induced metal−insulator transition is predicted in the NpV_2 SWN at 2+ charge state. We also find that the bonding strength between two nearest-neighbor metal atoms within one unit cell plays an important role in controlling the magnetic ordering in $NpTM_2$ SWNs (TM = Ti, V, Mn, Nb).

The first-principles calculations are performed using VASP code.[22,23] The projector augmented wave method[24,25] for the core region and spin-polarized density functional theory with the generalized gradient approximation (GGA) of the PBE functional[26] are used. A kinetic energy cutoff of 500 eV is chosen in the plane-wave expansion. To examine possible structural distortion in the SWNs, we set up a supercell containing two Np molecules and four metal atoms so that the initial structure is doubly repeated units of $NpTM_2$. Injection of electrons to the SWNs is simulated by adjusting the charge neutrality level, with a uniform jellium countercharge. Dipole correction to the total energy is considered in the calculations.[27] Two adjacent SWNs are separated by a vacuum region of 10 Å, and the 1D Brillouin zone is sampled by 20 special *k*-points. The conjugate gradient method is employed to fully relax the axial lattices and atomic positions until the force on each atom is less than 0.01 eV/Å. In addition, test calculations are performed by using the GGA+U method, and the results obtained are qualitatively the same.

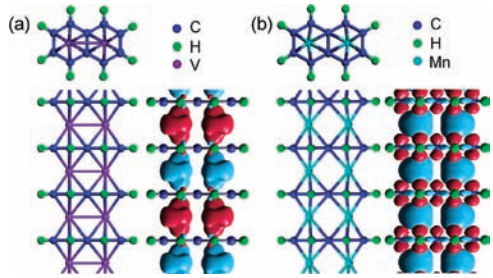

Figure 1. Top and front views of geometric structures, and the ground-state magnetization densities (0.2 e/Å^3) of (a) NpV_2 and (b) $NpMn_2$ SWNs. Magnetization densities in two spin directions are distinguished by light blue and magenta, respectively.

We have examined the $NpTM_2$ SWNs with the 3d TMs ranging from Sc to Cu and a 4d metal, Nb. We find that the Np molecules remain planar only for Sc, Ti, V, Mn, and Nb, while in other cases the two Np molecules in a supercell either form a nonzero angle with respect to each other or are structurally distorted (see Supporting Information, Figure S1, for details). Hence, Fe, Co, and Ni atoms are unsuitable for forming SWNs with Np molecules. This result supports a previous experimental finding that Fe, Co, and Ni favor forming rice-ball structures with benzene rings, rather than SWNs.[21,28] The $NpTM_2$ SWNs are AFM for TM = Ti, V, and Nb and FM only for TM = Mn, but nonmagnetic for TM = Sc. In view of the fact that only the NpV_2 SWN shows carrier-tunable ordering (shown later) and that Np_nV_m sandwich clusters have been synthesized, we focus on the NpV_2 SWN and use the $NpMn_2$ SWN for comparison.

The predicted most stable configurations of the NpV_2 and $NpMn_2$ SWNs are shown in Figure 1a,b. In both SWNs, each metal atom is chemically bonded to all six carbon atoms in a carbon hexagon, resulting in an η^6:η^6-coordination mode. The binding energies per V

[†] Nanjing University of Aeronautics and Astronautics.
[‡] University of Nebraska−Lincoln.
[§] University of Science and Technology of China.

and Mn atom in the SWNs are 4.17 and 1.62 eV, respectively, which are slightly smaller than those in the corresponding BzTM SWNs.[1] A notable structural difference between the two SWNs is that two nearest-neighbor V atoms form a weak bond but no bond is formed between the two nearest-neighbor Mn atoms, as shown by an analysis of electron localization function (Figure S2, Supporting Information).[29] This result is consistent with the fact that the Mn_2 dimer is difficult to produce.[30] To confirm thermal stability of the SWNs, we carry out a quantum molecular dynamics (MD) simulation in the canonical ensemble using a Nosé thermostat. The time step is set at 0.5 fs. For the MD simulation, we used a relatively large supercell consisting of six repeated nanowire units. At 400 K, we did not observe any signs of structure disruption during 5 ps MD simulation for neutral and charged NpV_2 SWNs (Figure S3, Supporting Information).

We now examine magnetic properties of the SWNs. Four initial magnetic configurations are considered for the four metal atoms in a supercell (one FM state and three AFM states, see Figure S4, Supporting Information). The NpV_2 SWN is an AFM metal. The local moments favor AFM coupling in the axial direction but FM coupling between the two nearest-neighbor V atoms (hereafter denoted as the AFM state), as illustrated in the right panel of Figure 1a. The energy difference between the FM and AFM states, $E_{FM} - E_{AFM}$, is only 11.5 meV per supercell. So the NpV_2 SWN probably exhibits a PM state at room temperature. In contrast, the $NpMn_2$ SWN shows a FM state (right panel of Figure 1b), and $E_{FM} - E_{AFM}$ is calculated to be −900 meV per cell (where the referenced AFM state is akin to that of NpV_2). The $NpMn_2$ SWN possesses a high charge spin-polarization of 56% near the Fermi level.

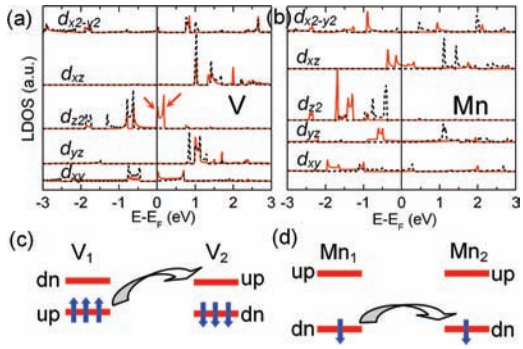

Figure 2. Projected LDOS for 3d orbitals of (a) V and (b) Mn in the $NpTM_2$ SWNs. Red solid lines denote the minority spin states, while black dashed lines denote the majority spin states. The red arrows in (a) denote splitting of the DOS induced by the nearest-neighbor V−V interaction. (c) Schematic energy levels for spin-up (up) and spin-down (dn) 3d states of two neighboring V atoms in the axial direction. The three arrows denote fully occupied level. (d) Schematic energy-level coupling diagram for FM interaction of Mn atoms in the axial direction. The single arrow denotes partially occupied level.

To gain more insight into the magnetic coupling, we computed the spin-polarized projected local density of states (LDOS) for the V and Mn atoms in the two SWNs (Figure 2). The C 2p states contribute little moment and thus are not discussed here. Due to reduced system symmetry, all the 3d orbitals of the metal atoms are nondegenerate, but crystal-field theory is not applicable here. In the case of NpV_2 SWN shown in Figure 2a, the minority of the spin states of d_{z^2} and d_{xy} orbitals are located just above the Fermi level, while a small fraction of $d_{x^2-y^2}$ states crosses the Fermi level, rendering the system an AFM metal. However, there are few electron carriers, as the V 3d states are either almost fully occupied or unoccupied, so the local moments favor AFM coupling due to a superexchange mechanism[31,32] (illustrated by the thick arrow in Figure 2c). Moreover, we observe a splitting of the LDOS peak in each 3d state as a result of the interaction between the two nearest-neighbor V atoms. This interaction decreases the intra-atomic exchange splitting so that the local moment on a V atom is 0.67 μ_B, which is mostly contributed by the d_{z^2} state. In contrast, for the $NpMn_2$ SWN, both the minority d_{xz} and majority d_{xy} states are partially occupied, giving rise to a large number of electron carriers. Hence, FM coupling among Mn spins in the axial direction is more favorable than AFM coupling because the hopping interaction between electrons in these states (denoted by the thick arrow in Figure 2d) is only allowed with parallel spin alignment. This is similar to the FM coupling in dilute magnetic semiconductors, such as (Ga,Mn)As[33] and (In,Mn)As.[34] The weak interaction between the nearest-neighbor Mn atoms results in a local moment of 1.02 μ_B on the Mn atom. In fact, the electron depletion from Mn atoms is smaller than that from V atoms in the formation of SWNs (see Figure S5, Supporting Information).

Since the AFM state in the NpV_2 SWN is due to insufficient electron carriers, we propose to inject electrons into the system to switch the nanowire to a FM ground state. Figure 3a presents $E_{FM} - E_{AFM}$ of the NpV_2 SWN as a function of the charge state. Indeed, the NpV_2 SWN rapidly turns into a FM ground state in negatively charged states. The $E_{FM} - E_{AFM}$ decreases with more negative charges and reaches −73 meV per supercell at the −2 charge state, sufficient for maintaining room-temperature ferromagnetism. The switching mechanism to the FM state can be understood from the LDOS shown in Figure 3b at the −1 charge state. It is clear that injecting electrons into the NpV_2 SWN makes the minority spin of tye V d_{z^2} state partially occupied. From the charge redistribution induced by the charge injection, we find that the injected electrons indeed mainly occupy the d_{z^2} orbital (inset of Figure 3a). The much increased electron carriers in the d_{z^2} state render the double-exchange mechanism[31−36] more effective than the superexchange mechanism so that the system has a FM ground state, similar to that in the $NpMn_2$. However, extra electrons in the system strengthen the in-plane V−V bonding, thus reducing the intra-atomic exchange splitting of the V 3d orbitals. Therefore, the local moment on V atoms decreases slightly with enhanced negative charge state, especially when the charge state is below −0.5 (e.g., 0.54 μ_B at −2 charge state). Due to the reduced local moment, the decrease of $E_{FM} - E_{AFM}$ at high electron injection levels is no longer as fast as that at low electron injection levels.

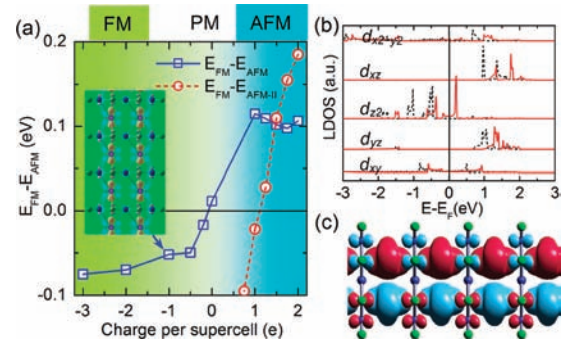

Figure 3. (a) Energy difference between the FM and AFM states, and between the FM and AFM-II states in the NpV_2 SWN as a function of the charge state. (Inset) Iso-surface plot (0.2 e/Å^3) of the charge accumulation at the −1 charge state with respect to neutral state. (b) Projected LDOS for 3d orbitals of V atoms in the NpV_2 SWN at −1 charge state. (c) Ground-state magnetization density (0.2 e/Å^3) of the SWN at +1.5 charge state.

On the other hand, $E_{FM} - E_{AFM}$ for the NpV_2 SWN is sharply increased in the +1 charge state, indicating that the AFM state can be increasingly favorable in positively charged states. A reason for this is that injecting holes into the system cannot induce sufficient carriers in the 3d orbitals, in particular in the d_{z^2} orbital that dominantly contributes the local magnetic moment. Instead, the injected holes will attenuate the in-plane V−V bonding so that local moment on V atoms is increased to 0.8 μ_B at the +1 charge state. The AFM state is thus further stabilized via enhanced hopping interaction between two adjacent metal layers. When the charge state exceeds +1.5, the local moments start to favor FM coupling between adjacent metal atoms in

the axial direction but AFM coupling between the two nearest-neighbor V atoms (Figure 3c). We name such a magnetic ordering as AFM-II. At the charge state of +1.5, the magnitude of local moment is 1.27 μ_B per V atom, notably larger than 0.91 μ_B in the AFM state. Since suppression of magnetic moment costs energy, the AFM state becomes less favorable. In fact, the nearest-neighbor V−V distance in the AFM-II state is larger than that in the AFM state by 0.07 Å (at +1.5 charge state). Interestingly, at higher charge state of +2, the NpV_2 SWN becomes a semiconductor with a direct band gap of 0.3 eV in the AFM-II ground state (Figure S6, Supporting Information), giving rise to a metal−insulator transition. The local moments of V atoms are now all different for two nearest-neighbor V atoms and for axially adjacent V atoms. For the two nearest-neighbor V atoms, one moment is 1.46 μ_B and another is −1.08 μ_B, but in the adjacent pair of V atoms, the corresponding moment becomes 1.08 and −1.46 μ_B, respectively. This semiconducting behavior is absent in other charge states and stems from the magnetic Peierls instability, which occurs when a half-filled band exactly crosses the Fermi level at the midpoint of the symmetry line Γ−X in the band structure of the SWN with the smallest cell (Figure S6).

The results shown above suggest that a PM-to-AFM or PM-to-FM transition can be induced in the NpV_2 SWN at room temperature by changing the charge state, which could be realized in reality either by using a field-effect transistor structure or by electrochemical doping. Note that the carrier-tunable magnetic coupling has been found to exist in finite-sized NpV_2 sandwich molecular clusters. For example, the magnetic coupling in an Np_3V_4 cluster can switch from the AFM state to FM one at the −1 charge state (see Figure S7, Supporting Information). Moreover, we found that the contact with metal electrodes does not affect the predicted carrier-induced switch of magnetic ordering in the Np_3V_4 cluster (see Figures S8 and S9, Supporting Information). By investigating the spin transport behavior for the Np_3V_4 cluster sandwiched between two Al electrodes under bias voltages, we observed distinct conductance in two spin channels for the cluster at both positive and negative bias, further supporting that the NpV_2 SWN exhibits spintronic characteristics upon electron injection.

Finally, we point out that the bonding between the two nearest-neighbor metal atoms plays an important role in controlling the magnetic coupling of charge-neutral $NpTM_2$ SWNs. The $NpNb_2$ SWN has stronger Nb−Nb bonding than V−V bonding in the NpV_2 SWN, and the calculated $E_{FM} - E_{AFM}$ is 40 meV per cell at the neutral state, with a local moment of only 0.42 μ_B on the Nb atom. Injecting electrons into the $NpNb_2$ SWN will reduce $E_{FM} - E_{AFM}$, but the AFM ordering is always the ground state regardless of the charge states. This is because the strong Nb−Nb bonding leads to a small intra-atomic exchange splitting that is less than the d bandwidth, which is unfavorable for double exchange.[34] In the $NpTi_2$ SWN, the bonding between two nearest-neighbor metal atoms is strongest among the $NpTM_2$ SWNs, and the SWN becomes a semiconductor with an AFM-II ground state. The local moment on the Ti atom is 0.9 μ_B in the AFM-II state but only 0.16 μ_B in the FM state and 0.07 μ_B in AFM state. As such, the AFM-II state in the $NpTi_2$ SWN is very robust to carrier doping.

We perform similar calculations for the $NpMn_2$ SWN and other types of SWNs, such as BzTi and BzV SWNs, but do not find carrier-induced switch of magnetic ordering. The carrier-tunable magnetic coupling seems to be unique to the NpV_2 SWN as a result of a delicate interplay between the intra-atomic exchange splitting and charge carriers, correlated with the V−V bonding.

In summary, we present theoretical evidence of carrier-tunable magnetic coupling in NpV_2 SWNs. To our knowledge, such a feature has not been seen in other sandwich nanowires, although control of the magnetization direction via oxidation state has been reported in $Eu_2(C_8H_8)_3$ clusters.[37] The default AFM ordering of the NpV_2 SWN can be switched to FM by injecting electrons, whereas injecting holes can further stabilize the AFM states. The ease of tunability, combined with predicted high stability, renders NpV_2 SWNs promising nanostructures for future electronic and spintronic applications.

Acknowledgment. We thank Prof. Jinlong Yang and Dr. Jing Huang for helpful discussions. X.C.Z. is supported by NSF (DMR-0820521) and the Nebraska Research Initiative, and by the University of Nebraska's Holland Computing Center. W.G. is supported by the 973 Program (2007CB936204), National NSF (10732040), and Jiangsu Province NSF (BK2008042) of China.

Supporting Information Available: Geometric properties for other $NpTM_2$ SWNs; three different AFM magnetization densities for the NpV_2 SWN; electron localization functions for the $NpTM_2$ SWNs; charge redistribution; band structure of the NpV_2 SWN at +2 charge state; magnetic modulation for finite-sized sandwich molecular clusters; snapshots of MD simulation; and transport property under bias voltage. This material is available free of charge via the Internet at http://pubs.acs.org.

References

(1) Xiang, H. J.; Yang, J. L.; Hou, J. G.; Zhu, Q. S. *J. Am. Chem. Soc.* **2006**, *128*, 2310–2314.
(2) Maslyuk, V. V.; Bagrets, A.; Meded, V.; Arnold, A.; Evers, F.; Brandbyge, M.; Bredow, T.; Mertig, I. *Phys. Rev. Lett.* **2006**, *97*, 097201.
(3) Koleini, M.; Paulsson, M.; Brandbyge, M. *Phys. Rev. Lett.* **2007**, *98*, 197202.
(4) Mokrousov, Y.; Atodiresei, N.; Bihlmayer, G.; Gel, S.; Blugel, S. *Nanotechnology* **2007**, *18*, 495402.
(5) Hosoya, N.; Takegami, R.; Suzumura, J.; Yada, K.; Koyasu, K.; Miyajima, K.; Mitsul, M.; Knickelbein, M. B.; Yabushita, S.; Nakajima, A. *J. Phys. Chem. A* **2005**, *109*, 9–12.
(6) Zhou, L.; Yang, S.; Ng, M.; Sullivan, M. B.; Tan, V. B. C.; Shen, L. *J. Am. Chem. Soc.* **2008**, *130*, 4023–4027.
(7) Shen, L.; Yang, S. W.; Ng, M. F.; Ligatchev, V.; Zhou, L.; Feng, Y. *J. Am. Chem. Soc.* **2008**, *130*, 13956–13960.
(8) Wang, L.; Cai, Z.; Wang, J.; Lu, J.; Luo, G.; Lai, L.; Zhou, J.; Qin, R.; Gao, Z.; Yu, D.; Li, G.; Mei, W. N.; Sanvito, S. *Nano Lett.* **2008**, *8*, 3640–3644.
(9) Mallajosyula, S. S.; Pati, S. K. *J. Phys. Chem. B* **2007**, *111*, 13877–13880.
(10) Wu, X.; Zeng, X. C. *J. Am. Chem. Soc.* **2009**, *131*, 14246–14248.
(11) Wang, J.; Acioli, P. H.; Jellinek, J. *J. Am. Chem. Soc.* **2005**, *127*, 2812–2813.
(12) Zhang, X. Y.; Wang, J. L.; Gao, Y.; Zeng, X. C. *ACS Nano* **2008**, *3*, 537.
(13) Kurikawa, T.; Negishi, Y.; Satoshi, F. H.; Nagao, S.; Miyajima, K.; Nakajima, A.; Kaya, K. *J. Am. Chem. Soc.* **1998**, *120*, 11766–11772.
(14) Kandalam, A. K.; Rao, B. K.; Jena, P.; Pandey, R. *J. Chem. Phys.* **2004**, *120*, 10414.
(15) Nagao, S.; Kato, A.; Nakajima, A. *J. Am. Chem. Soc.* **2000**, *122*, 4221–4222.
(16) Weng, H. M.; Ozaki, T.; Terakura, K. *J. Phys. Soc. Jpn.* **2008**, *77*, 014301.
(17) Burdett, J. K.; Canadell, E. *Organometallics* **1985**, *4*, 805–815.
(18) Pomije, M. K.; Kurth, C. J.; Ellis, J. E.; Barybin, M. V. *Organometallics* **1997**, *16*, 3582–3587.
(19) Ellis, J. E.; Blackburn, D. W.; Yuen, P.; Jang, M. *J. Am. Chem. Soc.* **1993**, *115*, 11616–11617.
(20) Elschenbroich, C.; Möckel, R.; Vasilkov, A.; Metz, B.; Harms, K. *Eur. J. Inorg. Chem.* **1998**, *1998*, 1391–1401.
(21) Kurikawa, T.; Takeda, H.; Hirano, M.; Judai, K.; Arita, T.; Nagao, S.; Nakajima, A.; Kaya, K. *Organometallics* **1999**, *18*, 1430–1438.
(22) Kresse, G.; Hafner, J. *Phys. Rev. B* **1994**, *49*, 14251–14269.
(23) Kresse, G.; Furthmuller, J. *Phys. Rev. B* **1996**, *54*, 11169–11186.
(24) Blochl, P. E. *Phys. Rev. B* **1994**, *50*, 17953–17979.
(25) Joubert, D.; Kresse, G. *Phys. Rev. B* **1999**, *59*, 1758–1775.
(26) Perdew, J. P.; Burke, K.; Ernzerhof, M. *Phys. Rev. Lett.* **1996**, *77*, 3865–3868.
(27) Makov, G.; Payne, M. C. *Phys. Rev. B* **1995**, *51*, 4014–4022.
(28) Jena, P.; Rao, B. K. *J. Chem. Phys.* **2002**, *116*, 1343–1349.
(29) Becke, A. D.; Edgecombe, K. E. *J. Chem. Phys.* **1990**, *92*, 5397–5403.
(30) Kant, E. A.; Lin, S. S.; Strauss, B. *J. Chem. Phys.* **1968**, *49*, 1983.
(31) Anderson, P. W. *Phys. Rev.* **1950**, *79*, 350–356.
(32) Dev, P.; Zhang, P. *Phys. Rev. B* **2010**, *81*, 085207.
(33) Mahadevan, P.; Zunger, A.; Sarma, D. D. *Phys. Rev. Lett.* **2004**, *93*, 177201.
(34) Akai, H. *Phys. Rev. Lett.* **1998**, *81*, 3002–3005.
(35) Zener, C. *Phys. Rev.* **1951**, *82*, 403–405.
(36) Sato, K.; Dederichs, P. H.; Katayama-Yoshida, H.; Kudrnovsky, J. *J. Phys.: Condens. Matter* **2004**, *16*, S5491–S5497.
(37) Atodiresei, N.; Dederichs, P.; Mokrousov, H.; Bergqvist, Y.; Bihlmayer, L. G.; Blugel, S. *Phys. Rev. Lett.* **2008**, *100*, 117207.

JA1029057